Dislocation studies on deformed single crystals of high-purity iron using positron annihilation: Determination of dislocation densities

Yong-Ki Park, James T. Waber, and Michael Meshii
Department of Material Science and Engineering, Northwestern University, Evanston, Illinois 60201

C. L. Snead, Jr.
Brookhaven National Laboratory, Upton, New York 11973

C. G. Park
Oak Ridge National Laboratory, Oak Ridge, Tennessee 37831
(Received 19 September 1985)

A new method for determining the total number of dislocations per unit area, as well as the fraction of screw and edge components, is presented. Single-crystal specimens which have been (a) bent over a mandrel, (b) cold rolled at room temperature, and (c) deformed in tension at 200 K have been studied. Etch pits were studied in connection with this work and were found to be primarily of the ⟨111⟩ type. The density of emergent dislocations as determined by the etch pits was found to be smaller than the number determined by the positron-annihilation technique.

I. INTRODUCTION

It has been recognized for some time that positrons can be trapped by dislocations before they annihilate, and that their lifetime[1–4] is similar to, but generally smaller, than the lifetime of positrons trapped at other defects such as a monovacancy.[5] Apparently the first observation of trapping in dislocations was made in 1964 by Dekhtyar *et al.*[1] This was followed in 1967 by Berko and Erskine[2] who studied the angular correlation of annealed and deformed aluminum and concluded that the positron would be localized on the dilatational side of a (edge) dislocation. This was before the introduction of the trapping model by Bergersen and Stott[6] and by Connors and West.[7] A number of studies followed. Doyama and Cotterill[3] listed the lifetimes for annihilation in the bulk and in dislocations for a number of metals, and these are generally quite close to the currently accepted values. Most of the detailed studies which involve positrons in metals have concentrated on vacancies and vacancy clusters.

A number of studies have recently been published[8–12] in which the annihilation characteristics of trapped positrons in cold-rolled metals are described in terms of the generic "dislocations" (by this phrase the authors mean a single trap component was fitted and labeled "due to a dislocation" when several types of dislocations were probably present) and alternatively in the case of iron, in terms of carbon-vacancy interactions,[13] and even in terms of trapping by self-interstitials by Frank *el al.*[14] There has been little agreement on whether the positron is localized in the vicinity of the dislocation or in its core, or by some other defect associated with a dislocation. This may reflect the general conviction best expressed by Siegel[15] that positrons will not readily bind to dislocations but only at jogs along them. It was reasoned that the lifetime in this trap should be similar to that of a vacancy. Doyama and Cotterill[3] were the first to argue that "once a positron arrives at the core of a dislocation, it diffuses very quickly [pipe diffusion] until it finds a vacancy attached to the dislocation or a jog of the dislocation, it is trapped and annihilates there." However, there is little convincing evidence today that pipe diffusion of positrons along dislocations is to be preferred conceptually over trapping on the dislocations line segment with no significant diffusion along the dislocation. Attention is directed in this paper to the effectiveness of trapping by edge and screw dislocations, and by the ability to determine the number of dislocations of each type per unit area.

II. EXPERIMENTAL PROCEDURE

A. Preparation of specimens

The single crystals of iron were prepared by a strain anneal technique.[16] The starting material was Materials Research Corporation MRC-VP grade (99.95 at. %) rod with an approximate diameter of 9.5 mm. The impurity content of a rod is presented in Table I. These single-crystal rods were cut in the electric-discharge machine (EDM) into disks, the thickness of which ranged from 0.3 to 1.2 mm. Tensile specimens were sliced along the rod axis and the final shape was produced with the EDM.

These specimens were mechanically polished with diamond paste and then with 0.03-μm alumina slurry. Next they were chemically polished in a solution of 80% hydrogen peroxide (30% aqueous solution), 5% hydrofluoric acid (48% aqueous solution), and 15% water. The dimensions of the tensile specimens in the gage area were 11×3.0 mm^2 and the range of thicknesses was between 0.4 and 1.1 mm. The polished samples were annealed and purified in a circulating ZrH_2 furnace at 1120 K for about 80 h. A thermodynamic argument was reported by Stein

TABLE I. Chemical analysis of the starting material MRC-VP grade iron as reported by the Materials Research Corporation. Values are in wt. ppm.

H	C	N	O	S	Mg	Si	Al	Ca
<1	18	<1	33	40	<10	50	60	<10
Ni	Cu	Ti	Cr	Mn	Ag	Sn	Pb	others
<10	30	<10	30	30	<5	<30	<30	no data

et al.[17] that the carbon, nitrogen, and oxygen contents should be almost undetectable after this treatment. More recently Meshii and coworkers[18] reported that the content of interstitial impurities such as C and N could be reduced substantially more than the O content.

Annealed, bent, and cold-rolled single-crystal specimens of Fe were measured at room temperature. For some of the above specimens that were deformed at low temperature, measurements were made at liquid-nitrogen temperature using a specially designed Dewar in order to retain the as-deformed dislocation structure. Some of the disk-shaped specimens were bent at room temperature over mandrels with differing diameters. Deformation by tension was carried out in a dry ice and methanol bath at 200 K with a strain rate 1×10^{-4} sec.$^{-1}$ Shortly after deformation, the specimens were quenched into liquid nitrogen.

B. Positron-lifetime measuring system

Positron lifetimes were measured by a fast-fast system. This system measures the time interval between (i) the arrival of the first γ ray of 1.28 MeV which is emitted from the ^{21}Ne nucleus about 10 psec after the positron is emitted from the ^{22}Na nucleus and (ii) the detection of one of the two 0.511-MeV γ rays which results from the annihilation of the electron-positron pair.

The positron source was prepared from an aqueous solution of ^{22}NaCl which was evaporated onto a thin titanium foil ($\sim$1.13 mg/cm^2), covered with a like foil, and then sandwiched between two identical specimens. This sandwich was held in place by wrapping it in aluminum foil. Since the two γ rays from ^{60}Co are emitted at nearly the same time, the measured time spectrum using them as start and stop is a close approximation of the prompt resolution curve.[19,20] Since the energy spectrum of ^{22}Na is different from that of ^{60}Co, there might be some deviation between the natural resolution and the measured prompt curve using ^{60}Co.[21,22]

Figure 1 shows the time spectrum measured with ^{60}Co and the fitted function (the prompt curve extracted from the spectrum in the fitting routine) in well-annealed iron single crystals with ^{22}Na. The resolution function we used was a Gaussian with a double-sided exponential.[23,24] The full width at half maximum (FWHM) of the ^{60}Co spectrum is 299 psec and that of the ^{22}Na is 301 psec.

In order to test the timing system further, the lifetime of ^{207}Bi was measured. This isotope is known to be an excellent standard, since it emits two γ rays of 1.06 and 0.57 MeV, which are similar to the γ rays of ^{22}Na, and the lifetime of the metastable state is 187 psec.[25,26] Moreover, there is no source component to subtract from the experimental spectrum when using ^{207}Bi which might cause error in the positron-lifetime measurement. A 21.4-μCi ^{207}Bi source was placed between two scintillators and the time spectrum was collected without changing the settings of the lifetime system (^{22}Na windows). Figure 2 shows the variation of the lifetime (actually the time difference) and χ^2/ν as a function of the right-hand slope of the resolution function (R). The lifetime decreases as R is increased because a larger fraction of the time spectrum is deconvoluted as a resolution function. The χ^2/ν parameter has a minimum for R values around 45 psec and increases rapidly if R is increased further. If we choose the minimum value of the χ^2/ν condition for the best slope, the time difference between the generation of the two γ rays in ^{207}Bi is 185$\pm$0.5 psec which is in quite good agreement with MacKenzie's value.[25,26]

A fitted value of R less than 45 psec would, in general, be acceptable as causing a minimum uncertainty in the

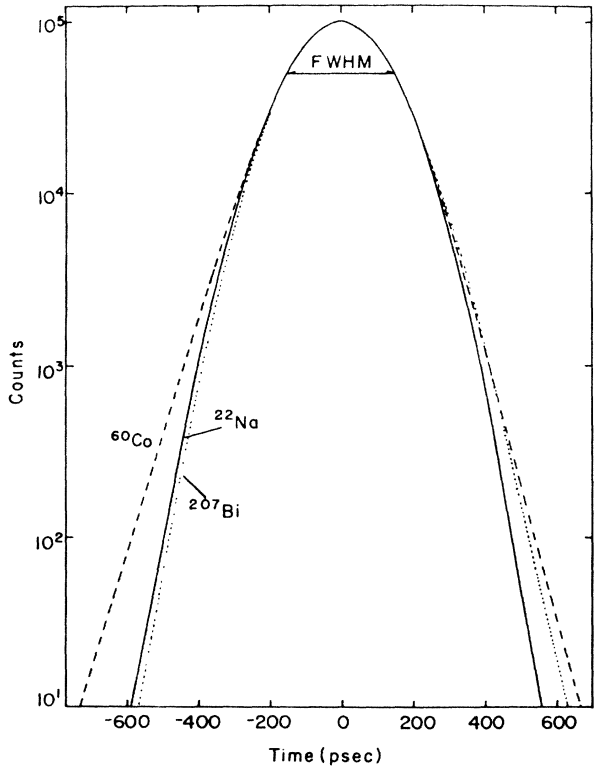

FIG. 1. Measured resolution function obtained with ^{60}Co and the fitted prompt curves (extracted from the spectrum in the fitting routine) measured with ^{22}Na and ^{207}Bi.

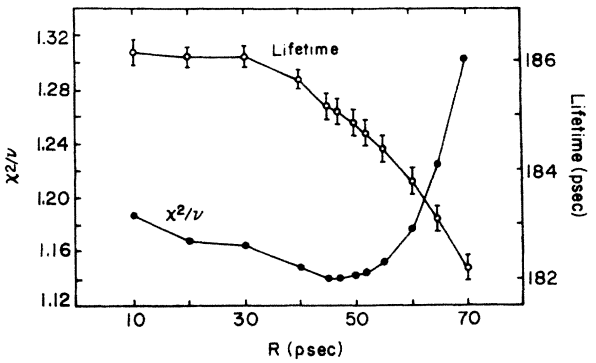

FIG. 2. Variation of the lifetime and χ^2/ν as a function of the right-hand slope of the resolution function R for ^{207}Bi.

measured lifetime. Therefore, in analyzing the lifetime spectra the initial value of R was chosen near 45 psec, and the other parameters were initialized using the values obtained with ^{207}Bi. The resolution function obtained with the ^{207}Bi spectrum is similar to that for ^{22}Na.

1. *Treatment of the lifetime data*

The intensity of a component of the lifetime spectrum due to a particular trapping site (in which the positron lifetime is $1/\lambda_T$) is given by the expression[27]

$$I_T=\frac{\kappa_T}{\lambda_b-\lambda_T+\sum\kappa_j}\ , \tag{1}$$

where

$$\kappa_T=\mu_T C_T\ . \tag{2}$$

Here κ_T is the positron trapping rate in the specific trap, $1/\lambda_b$ is the lifetime in the bulk, μ_T is the specific trapping rate for the trap, C_T is the trap concentration, and the summation runs over the trapping rates of all the j traps. It is the ability to resolve the various I_T's associated with the various traps present that allows a meaningful study of multiple-trap systems.

A source component was subtracted from the spectrum before fitting the data with the trapping model.[6,7] When the specimen was not in the liquid-nitrogen Dewar, the source component was 340 psec with an intensity of $\sim$5.5%. When the annihilation spectrum was measured for a specimen at 77 K in the Dewar, the source component increased to 570 psec with an intensity of $\sim$8%.

2. *Reproducibility and accuracy of the system*

More than 10^6 counts were taken in almost all of the experiments to ensure low values of χ^2/ν. The positron lifetimes obtained (assuming only one trap) for a repetition of runs with the same specimen differ only by 2 psec, and results of measurements on different specimens vary within the same range. The mean of all the lifetime determinations for annihilation in the trap-free bulk is 114$\pm$2 psec. This value is in good agreement with four independent values reported for iron, namely 117 psec reported by Doyama and Cotterill,[3] 111 psec by Cao Chuan *et al.*,[28] 110 psec by Hautojarvi and co-workers,[12,13] and 108 psec by Van Brabander *et al.*[10]

As a further check on the compatibility of the two-lifetime systems used, well-annealed, high-purity aluminum specimens were measured at Northwestern University and at Brookhaven National Laboratory. The two lifetimes were 164.1$\pm$3.7 and 162.5$\pm$1.6 psec, respectively. Not only are these two values very close to each other, they are in excellent agreement with the reported value for Al of 163 psec by Schultz *et al.*,[29] and of 161$\pm$2 psec by Hall, Goland, and Snead.[30]

C. Doppler-broadening measuring system

The line shape of the Doppler-broadened γ rays from positron annihilation was measured with a high-purity germanium detector (Ortec model No. GEM-10175). The energy resolution (expressed as FWHM) was 1.70 keV at an energy of 1.33 MeV from ^{60}Co.

The Doppler-broadened line shape was analyzed using line-shape parameters after subtracting the background expressed as a two-sided error function discussed by Jorch and Campbell.[31] In simplified line-shape analysis, the Doppler spectrum is not fitted, but areas under the curve in limited energy ranges are compared. The peak-to-wing parameter P/W used here is the ratio of the area under the central 19 channels to the area of the two wing portions centered 38 channels on either side of the peak channel. The absolute value of P/W is larger than P and, hence, is more sensitive to changes in the defect concentration. A small amount of algebraic manipulation will show that the P/W is the ratio of two linear functions of the defect concentration, and thus is in fact a linear function of the latter (to the first approximation) with a small remainder. Byrne and co-workers[32] found that P/W is a linear function of the density of dislocations measured by x-ray line breadth. If a specific value exists for both the peak and the wing for a given type of trap, then a $(P/W)_j$ exists for the jth type of trap, and one can form a linear combination of these values.

The trap concentration C_T can be expressed[27] by another equation:

$$C_T=\frac{\lambda_b(F-F_b)}{\mu_T(F_T-F)}\ , \tag{3}$$

where F is any characteristic property or parameter of the positron annihilation process which is a linear function of the positron state. Then F_T and F_b are F values of the trap and trap-free bulk, respectively.

The line shape was found to be dependent on the counting rate as was observed recently by Nielsen.[33] As the counting rate decreased, the value of P increased. However, these changes became very small when the total counting rate was near 2×10^3 sec^{-1}. This counting rate was adopted.

III. RESULTS

A variety of results are reported in this section such as the lifetimes of the two basic types of dislocations as well as the results of etching the specimens to develop etch pits and counting them by means of replicas examined in a transmission electron microscope.

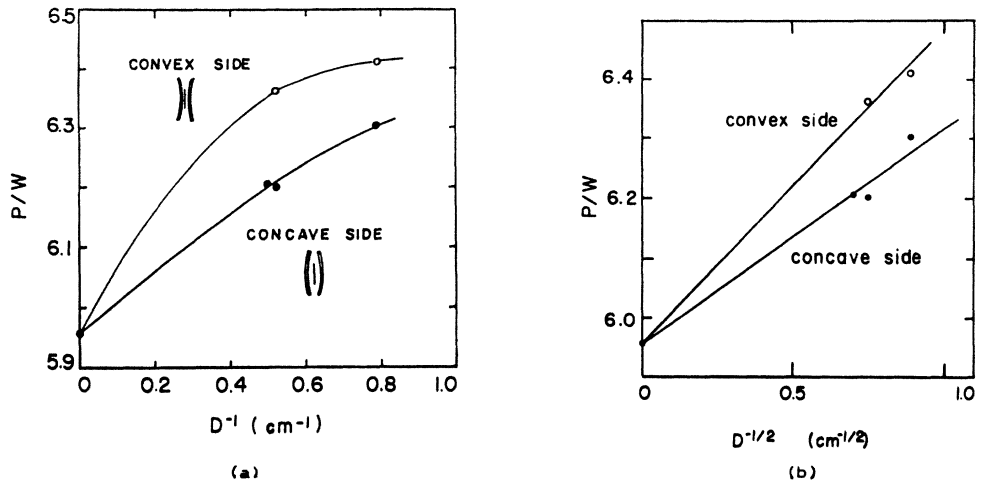

FIG. 3. Doppler-broadening line-shape parameter for bent iron crystals: (a) P/W parameter as a function of the curvature (reciprocal of the mandrel diameter), (b) the same parameters as a function of the square root of the curvature. The error bar is the same size as the marks. Solid lines are guides to the eye.

A. Cold-bent specimens

Single-crystal specimens were bent to a fixed diameter by means of a machined cylinder mating a fixed mandrel. The concave and convex sides of the bent specimens were studied separately. In Fig. 3(a) typical results are plotted versus D^{-1}, and in Fig. 3(b) versus the square root of D^{-1}, where D is the diameter (of curvature) of the mandrel used, which in turn is linearly dependent on the strain. Because of the formation of redundant dislocations during the deformation, the number on either side should not be expected to be as small as the minimum number of dislocations needed to produce the curvature. The latter depends on the net number of dislocations. The single-lifetime fit of the dislocation traps gave a value of 165±5 psec. The densities determined for the two sides of a specimen are presented in a later section.

B. Cold-rolled specimens

Some of the early results for cold-rolled single-crystal specimens are presented in Fig. 4(a). The y axis of the left-hand panel is the peak-to-wing parameter P/W from the Doppler-broadening measurements. The fraction of positrons annihilating in the "trap" I_2 is shown in the right-hand side of Fig. 4(b). The lifetime in this trap was 155±3 psec. In contrast to the lifetime found for the cold-rolled specimens, the single lifetime in traps of the bent specimens was 165±5 psec. It thus becomes apparent that the lifetime difference for the two types of deformation is reflecting a different distribution of the types of traps present after the deformations. Reasonable linearity is exhibited for small strains when the trapping rate κ_T is plotted versus the square root of the strain as is shown in Fig. 5, where the P parameter from the

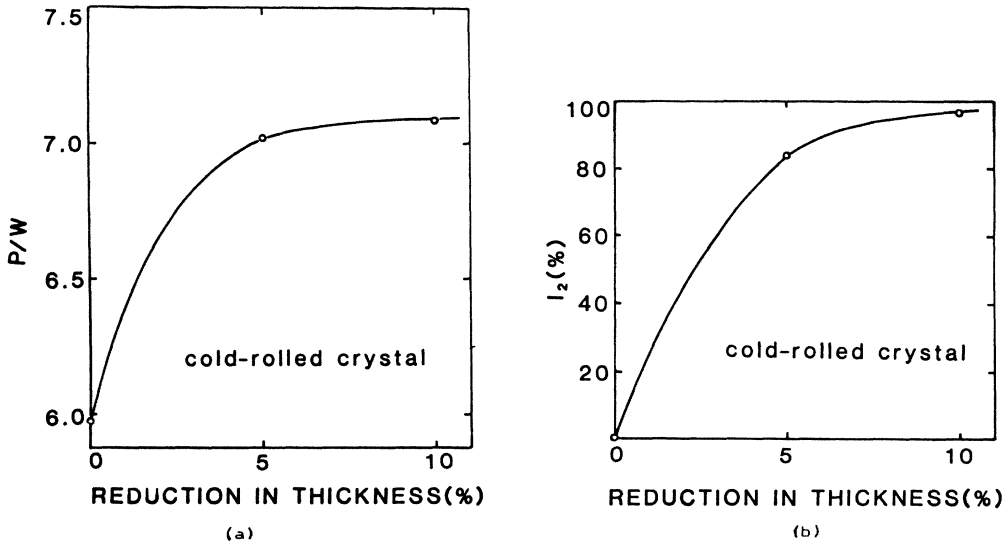

FIG. 4. Positron annihilation measurements on cold-rolled iron: (a) the peak-to-wing (P/W) parameter of Doppler broadening, (b) the fraction of the positron annihilating in the trap with the lifetime 155 psec. The error bar is the same size as the marks. Solid lines are guides to the eye.

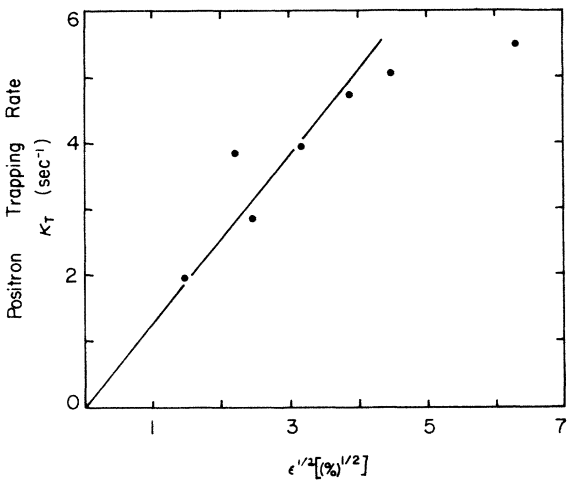

FIG. 5. Positron annihilation rate in the defects of cold-rolled iron single crystal 2 as a function of the square root of the deformation, namely the reduction in thickness. The error bars are the same size as the points plotted.

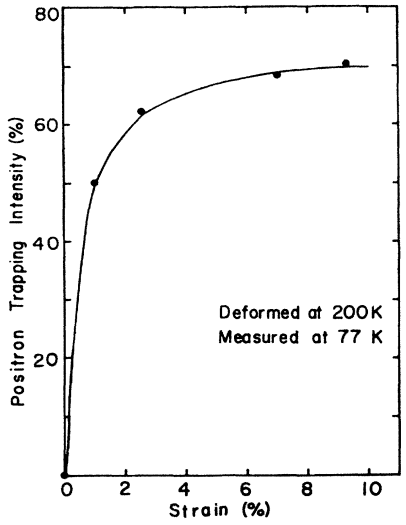

FIG. 7. Total fraction of the positrons annihilating in traps at 77 K of single crystals 1 deformed in tension at 200 K.

Doppler-broadening data for the cold-rolled specimen was used. The trap concentration variation with strain will be discussed in detail later.

C. Effect of tensile deformation at dry-ice temperature

There is general agreement[34,35] that screw dislocations are produced primarily in high-purity iron samples which are deformed in tension at 200 K or lower. We investigated the possibility that the annihilation rate in screw dislocations might be different from that of an edge.

Stress-strain curves for two different orientations of Fe single crystals are shown in Fig. 6. There is some evidence of a weak yield point. The inset shows the orientation of the single-crystal sheets. The orientation of zone-refined single iron crystals used by Kimura and Kimura[36] was slightly different but showed quite similar stress-strain behavior. When the lifetimes from these specimens were analyzed, the value of approximately 142 psec (for a single-trap fit) emerged. It is important to note that the fraction of positrons annihilating in this trap increased monotonically with the tensile strain.

The fraction of positrons annihilating at 77 K in the traps created by deformation is plotted (for a single-trap fit) versus strain ϵ in Fig. 7. Using a two-trap model, two curves of κ_T are presented in Fig. 8; one for 142 and the other for the 165 psec components resolved. As noted above, the relative trapping rates κ_T are directly proportional to each dislocation density ρ_T. As has been reported by Kubin,[37] the number of edge components rises initially more rapidly than the number of screw components for low-temperature tensile deformation, and as observed here, after about 3% elongation this situation reverses and further deformation of iron at 200 K produced mainly screw dislocations. In the absence of any definitive information about the specific trapping rate from dislocations, the authors used an "average" value of the specific trapping rate μ_T to estimate total density of dislocations. Subsequently the specific trapping rates for the edge and screw dislocations were handled separately.

The smaller dilatational field, *vide infra*, around the

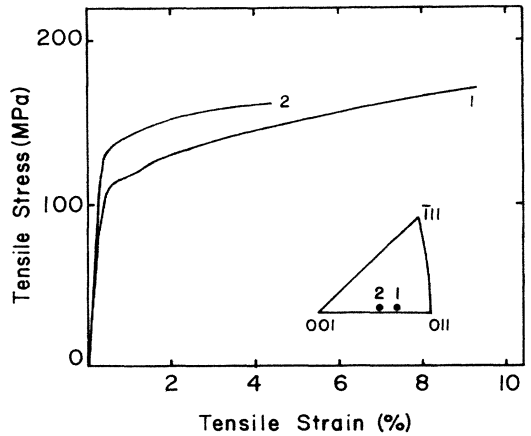

FIG. 6. Stress-strain curves of iron single crystals deformed in tension at 200 K.

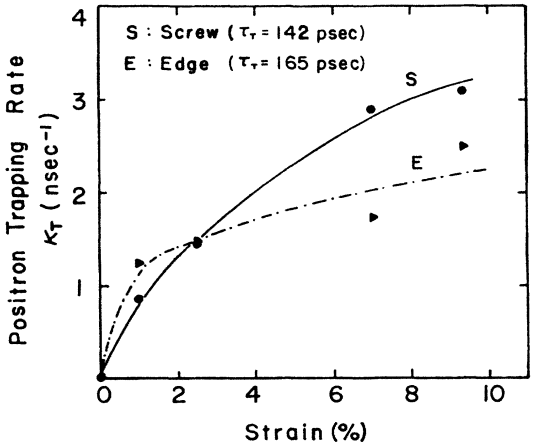

FIG. 8. Positron trapping rates at 200 K in edge and screw dislocations in single crystal 1 deformed at 200 K in tension.

core of the screw dislocation compared to that of an edge dislocation,[38] would suggest that μ_T would probably be smaller for the screw components. Consequently the number of screw dislocations would be relatively even larger than Fig. 8 would imply. There appears to be general agreement among electron microscopists that the collection of screw dislocations formed at 200 K in iron becomes motionally (mechanically) unstable when the temperature approaches room temperature. Crystal 2, after straining 4.5%, had a ratio of the two trap intensities of 4.5 (using identical specific trapping rates). The specimen that was deformed at 200 K was permitted to warm up and was kept for 48 h at 300 K. Upon measuring the lifetime spectrum again at 77 K, the ratio of I(screw) to I(edge) decreased to 1.5. This is certainly consistent with the anticipated disappearance of screw components.

In order to confirm further the suspected recovery of the screw dislocations with which we associate the disappearance of the 142-psec lifetime component, a series of internal-friction measurements were performed. Specimens for vibrating-reed measurements were spark cut from the same stock the positron specimens came. Standard phase-locked-loop and capacitive-pickup techniques were used for fundamental-mode vibrations of ~ 500 Hz. Specimens were pulled in tension to strains of 3.5% and 10.1% at 200 K. They were mounted cold and the internal friction monitored for consecutive runs from 6 to 350 K.

For Fe deformed below room temperature it is well established that there is an internal friction peak near 30 K (the α peak) which is associated with double-kink formation on nonscrew dislocations, and a peak near 300 K due to double-kink formation on screw dislocations.[39] We first made measurements on a crystal that was annealed and undeformed. There was a monotonic increase of the internal friction Q^{-1} with temperature with no structure present (data not shown). For the specimen deformed to 3.5% at 200 K the two runs to 350 K are shown in Fig. 9. In the first warmup following the deformation, both the α and the γ peaks are present. Following the first warmup, the holding at 350 K for 1 h, the second warmup shows the disappearance of the γ peak that is associated with the screw dislocations. Similar results are obtained with a specimen deformed to 10.1% at 200 K and shown in Fig. 10. (The peaks at ~ 140 K are probably due to defect-dislocation interactions.) For both deformations it is clear that the anneal above room temperature suffices to remove the screw dislocations which are the cause of the γ peak, and which also coincides with the disappearance of the 142-psec lifetime component as discussed above.

Low-temperature-deformed single-crystal sheet specimens were examined by etch-pit techniques. The same specimens from crystal 1, which had been measured by positron annihilation, were chemically polished in a solution of 80% hydrogen peroxide (of 30% aqueous solution), 5% hydrofluoric acid (48% solution), and the balance water. Then they were etched in the potassium sulfate + sulfuric acid mixture recommended by Shemenski, Beck, and Fontana.[40]

In order to resolve the individual etch pits so they could be counted, the etching time was reduced to 20 sec. A two-stage carbon replica was made of the etched surface and the former shadowed. The increase in the number density of pits with increasing strain as photographed in a transmission electron microscope can be seen in Fig. 11. In counting the etch pits, enlargements of the original photographs were used. Pictures were prepared from several different areas of the specimens and the average number of pits was divided by the area in the photograph. This number was taken as the total dislocation density. Results are presented in Table II and the data are plotted in Fig. 12 to show the linear dependence on the true strain.

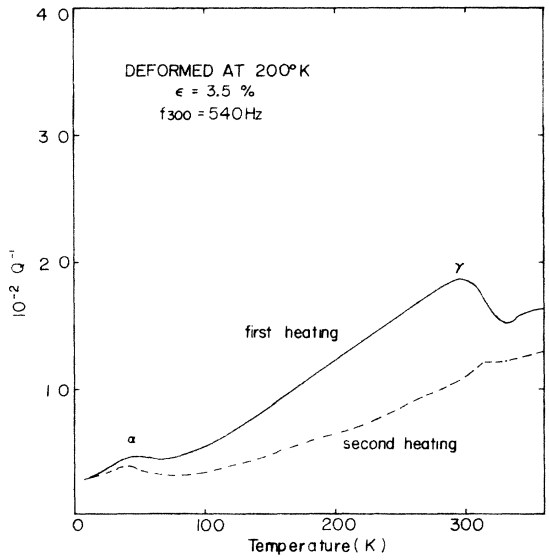

FIG. 9. Internal friction of the iron single crystal deformed by tension at 200 K. Second heating was measured after annealing at 350 K for 1 h.

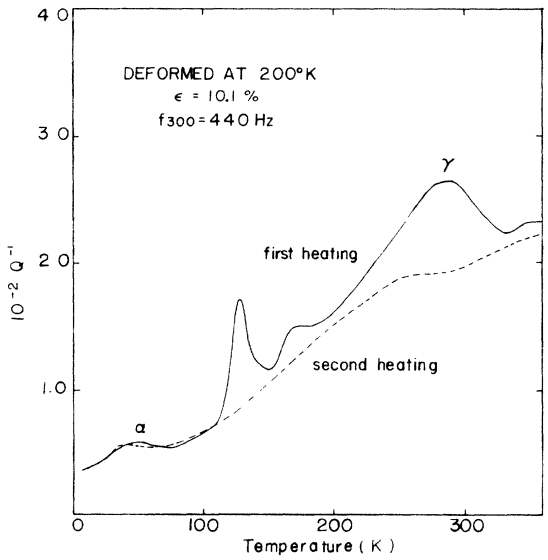

FIG. 10. Internal friction of the iron single crystal deformed by tension at 200 K. Second heating was measured after annealing at 350 K for 1 h.

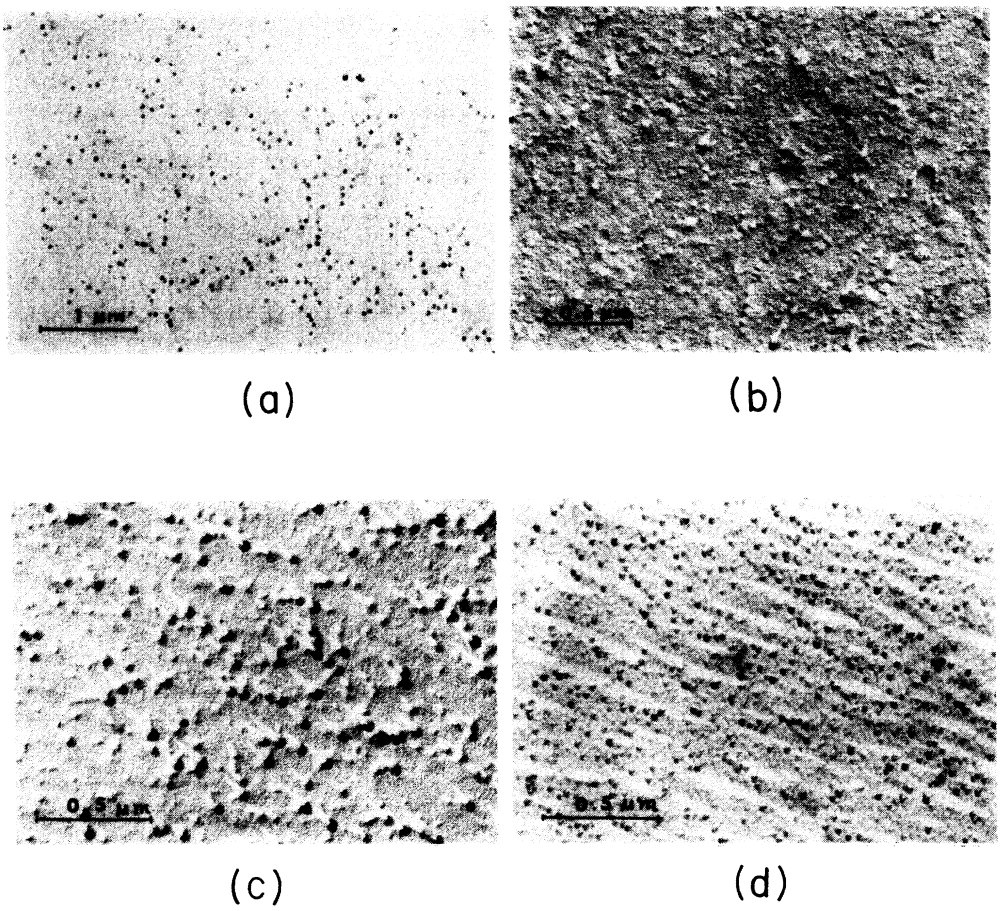

FIG. 11. Transmission electron micrographs of replicas of the etch pits developed on the surface of iron single crystal 1 deformed in tension at 200 K for increasing amounts. (a) $\epsilon=1.0\%$ strain, (b) $\epsilon=2.5\%$, (c) $\epsilon=7\%$, and (d) $\epsilon=9.3\%$.

IV. ANALYSIS OF THE DATA: DETERMINATION OF DISLOCATION DENSITY

This section consists primarily of the determination of the specific trapping rates after the number of dislocation of the edge and screw types had been determined.

In Eqs. (2) and (3) above, a trap concentration can be calculated if the specific trapping rate μ_T for a specific kind of a trap is known. Unfortunately there are no published values of the specific trapping rates for dislocations in iron. The present concomitant measurements of both the Doppler profile and the lifetime on the same specimen offer the possibility of using the two equations to deter-

TABLE II. Dislocation densities in iron crystal 1, deformed at 200 K which were obtained from etch-pit counts.

True strain (percent)	Dislocation Density (10^{13} m^2)
1	2
2.5	5
7.0	7
9.3	9

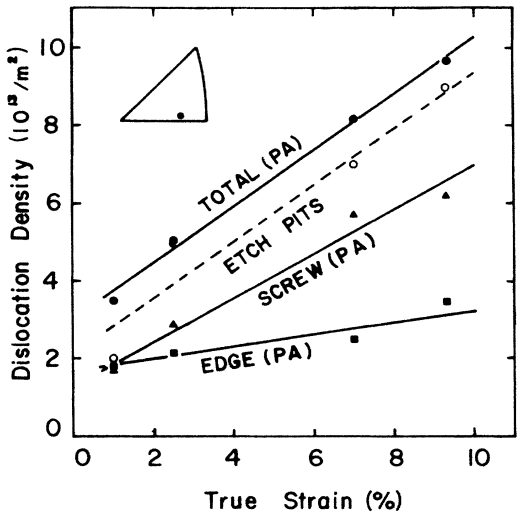

FIG. 12. Dislocation density in iron single crystal 1, which was deformed in tension at 200 K. Solid circles represents the total dislocation density as measured by positron annihilation and open circles are the values from the etch-pit measurements. Triangles and squares represent the edge and the screw components measured with positron annihilation.

mine two unknowns. Note that κ_T in Eq. (2) can be determined from positron-lifetime spectra, and F can be replaced by the P parameter determined from the Doppler-broadened line shape to yield a second value.

We have estimated the specific trapping rates for the dislocation species in cold-rolled specimens in the following manner. Yamakawa *et al.* reported the dislocation density in pure iron[41] and in low-carbon steel.[42] Their specimens were deformed at room temperature and measured by electron microscopy, x-ray line broadening, and hydrogen permeation. Their results were internally consistent. Since it is difficult to locate this journal,[41,42] their data are replotted in Fig. 13. They also separated the densities of edge and screw dislocations based on the profile of certain x-ray diffraction lines.

In the following calculation, the total dislocation density was deduced from their values obtained by electron microscopy that were carried out at the same two levels of strain in both our work and in Yamakowa *et al.* In addition, the ratio of screw to edge dislocations was also obtained from their x-ray results. By using the total dislocation density for the 5% and 10% deformations from Yamakawa *et al.*,[41,42] with the present values of κ_T determined in our lifetime spectra, the specific trapping rate for a generic or average dislocation was calculated. This is a reasonable assumption to make initially in the absence of any prior determination. The total density was then calculated from the P parameter data of the Doppler-broadened lines from the same two specimens using the average μ_T just obtained. When lifetime data are used, two trapping rates κ_T (one for edge and the other for screw) can be deduced. The concentration or density is inversely proportional to the specific trapping rates μ_T.

The Doppler-broadening data are represented by one (or at best two) simple shape parameters. These are capable of yielding the average (total) dislocation density, but without detailed deconvolution of the broadened line, discrimination between edge and screw dislocations is not possible. Therefore, other data, external to the position annihilation data, are needed to separate the two specific trapping rates μ_T, from the combined or total density of dislocations. The numbers of edge and screw dislocations were then estimated using the ratio given by Yamakawa *et al.* Thus two trapping rates were separated for the edge and screw components. In this way, the data were normalized. These results are presented in Table III. The sum of the second and third columns agrees well with the

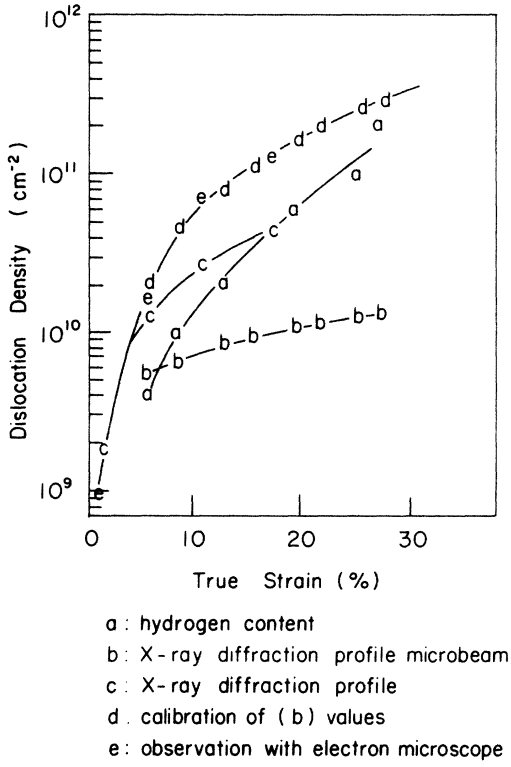

FIG. 13. Dislocation density as a function of the true strain measured by various methods [from Yamakawa *et al.* (Ref. 41)].

total density observed by Yamakawa. The two specific trapping rates in the fourth column and in the fifth column are similar. Average values of 5×10^{-5} and 7×10^{-5} m^2/sec can be used for other determinations of screw and edge components. As was anticipated, the specific trapping rate we have obtained for a screw dislocation μ_s is smaller than that for an edge dislocation μ_e. Kuramoto *et al.*[43] also briefly discussed that such a result would be reasonable to expect.

These specific trapping rates were used with their respective κ_T values to estimates the dislocation densities of iron single crystals produced in two ways, both in bent specimens and in those deformed at low temperature. The specific trapping rate for an edge dislocation was used in calculating the dislocation density in bent specimens as shown in Table IV, the dislocation density on the convex side (tension side) is somewhat higher than on the concave

TABLE III. Specific trapping rates for edge and screw dislocations in iron single crystals.

Deformation	Density of screw dislocation[a] (m^{-2})	Density of edge dislocation[a] (m^{-2})	μ_s[b] (m^2/sec)	μ_e[c] (m^2/sec)
5	0.9×10^{14}	0.6×10^{14}	6.1×10^{-5}	7.8×10^{-5}
10	3.3×10^{14}	1.7×10^{14}	4.0×10^{-5}	6.2×10^{-5}
average			5.1×10^{-5}	7.0×10^{-5}

[a]Obtained from the total dislocation density and the ratio of screw and edge component reported by Yamakawa *et al.* (Ref. 41).

[b]The specific trapping rate in the screw dislocation.

[c]The specific trapping rate in the edge dislocation.

TABLE IV. Calculated total density of dislocations in bent single crystals of iron (in units of 10^{13} m^{-2}). (Lifetime observed was 165±5 psec.)

Diameter of mandrel (mm)	Concave side	Convex side	Difference
50.8	1.0	1.5	0.5
20.2	1.3	2.5	0.8
19.1	2.0	3.3	1.3
12.7	2.9	3.9	1.0

side (compression side). An excess is to be anticipated since the curvature of the specimen depends on it.

It has been reported[44] that in the early stages of deformation there is a linear portion in the relationship between the dislocation density and the strain. This linearity was satisfied up to at least a true strain of ~10%.[44,45] We note that the total dislocation density measured by the etch-pitting technique is somewhat lower than that measured by positron annihilation (see Fig. 12). However, the slopes of the total density versus strain curves are quite similar to each other. In interpreting the etch-pit technique some of the dislocations might not be revealed because a short etching time was used to increase the resolution, and therefore the actual dislocation density could be higher than the number of etch pits. When this is considered, the total dislocation density measured by positron annihilation is considered to be in very good agreement with the density as inferred from the etch pits.

In Fig. 12 the slope of the screw component is similar to that of the total dislocation density but the edge component has a much smaller slope, which implies that the screw dislocation concentration is dominant during deformation at this temperature.

V. DISCUSSION

Several subjects are taken up under this heading. First is the question of ultimate trapping of the positrons at dislocations versus jogs, which is central to this investigation. Next is the resolution of two different lifetimes for the dislocation components is discussed. The specific trapping rate the authors obtained is compared with values which were previously reported but not emphasized. Then some results obtained by others are summarized. General suggestions for further work are given.

A. Discussing jogs versus dislocations

In 1979 Doyama and Cotterill,[3] referring to their paper, stated, "There is not much of an opening of ions at the core of the dislocations. Therefore positrons probably do not annihilate at the normal sites of the core of the dislocations." In their Fig. 1 the arrangement of atoms on three consecutive (112) planes does not indicate much dilation around the screw dislocation. However, by using anisotropic elasticity theory, an alternating threefold dilatational field is indicated for a screw dislocation.[36] Although the dilatational field is 60—70% smaller than around an edge dislocation, it is still appreciable.

Doyama and Cotterill,[3] to make the point, illustrate the constriction of dislocation ribbons associated with the formation of a jog. The drawing appears to be applicable to face-centered-cubic metals. However Argon and Moffatt[46] have shown the atomic positions near an acute jog in a body-centered-cubic metal. One can see appreciable "spaces" which occur that are similar to those along the edges of the ribbon.

Smedskjaer, Manninen, and Fluss[47] suggested that there is insufficient interaction between a (edge) dislocation and a "positron to trap the latter long enough to increase its lifetime." It was more probable, in their opinion, that the dislocation would serve as temporary storage and that diffusion of the positron would occur readily along, or parallel to, the dislocation core until the positron came under the influence of a jog. They suggest that the jogs might be 100—1000 Burgers vector lengths B apart. The latter (jogs) would be expected to form by dislocation-dislocation interactions—mainly by one dislocation cutting across another, i.e., to form when the dislocation density becomes high. Cross slip could also produce this type of jog. While they presented a kinetic analysis to show that certain phenomena could be explained by means of their model, there has been very little direct evidence presented to support this concept.

Admittedly most of the positron studies have been carried out in the past after a substantial reduction in thickness has occurred; i.e., after 20—50% cold work it would be very likely that complex dislocation arrangements would be observed with the electron microscope. In fact, there appears to be a paucity of confirmatory examination of specimens in the transmission electron microscope either before or after submitting these specimens to positron annihilation.

The positron may be "trapped" but not immobilized within the core of the dislocation. It does not escape, it merely finds a deeper trap somewhere along the dislocation at, for example, a jog. This implies high positron-migration velocities down the core. While it is well demonstrated that the diffusion of substitutional atoms is facilitated by pipe diffusion along a dislocation, there seems to be much less convincing evidence for pipe diffusion of interstitial atoms (other than self-interstitials.) There is evidence that hydrogen is transported by moving dislocation during straining,[48—50] but not *along* the dislocation.

There is evidence that positrons can be trapped at dislocations with sufficiently low binding energies that sites other than jogs, which are considered deep traps, are indicated. Smedskjaer *et al.*[47] calculated a binding energy to a "perfect" dislocation line for positrons of 0.1 eV. Snead *et al.*[51(a),51(b)] found the value of 0.1±0.05 eV for the binding of positrons to shallow traps (dislocations) in Mo. The release of positrons from these traps upon warming between 77 and 300 K demonstrates the possibility that, at least at low temperatures, the positron is trapped on the dislocation and not in the deeper jog traps. For trapping at screw dislocations, the same low binding energy might cause detrapping if the measurements were carried out at higher temperature. Our measurements were at 77 K where such detrapping effects should be minimized.

Low and Turkalo[52] studied dislocation multiplication in silicon-iron single crystals using a transmission electron microscope. In specimens deformed by compression, at 1% the number of jogs in a 1 cm length of screw dislocation was approximately 2×10^4. This means that the average distance between jogs is about 0.5 μm, and the concentration of jogs in the specimen in which the density of dislocations is 5×10^{13} m^2 reduces to 1.2×10^{-9} per Fe atom. This frequency of jog occurrence is very similar to the number which Smedskjaer *et al.*[47] used, namely a jog every hundred $|B|$ along the dislocation. Even if the jog is assumed to have ten times higher trapping capability than a monovacancy this concentration is too small to be of any significance in direct positron trapping. The lower limit for detection of vacancy concentration is of the order of 0.1 ppm (Ref. 53) with currently available equipment. Jogs of this separation and density could only play a role if, as Smedsjkaer *et al.* postulate, the positron localizes on the dislocation line and rapidly diffuses along it to the jogs. The rate-limiting step in the ultimate trapping state of the positron does not then involve the cross section of the jog *per se,* but rather the trapping cross section of the dislocation line itself. This concept of increasing the efficiency of a trap by reducing the dimensionality of the diffusion process is nicely demonstrated by Adam and Delbrück.[54] It should also be kept in mind that the above estimations of jog densities are based upon transmission-electron-microscopy (TEM) observations. Nothing has been said about the possible existence of high concentrations of jogs with atomic dimensions that are below the resolution of TEM studies.

B. Direct observation of dislocation structure

Thin foils were prepared from low-temperature deformed and room-temperature cold-rolled specimens. Disk specimens were cut by an electric-discharge machine (EDM) and were thinned in a fresh solution of hydrogen peroxide and hydrofluoric acid. The final thinning beyond 0.15 mm was done by jet polishing in a dry-ice and methanol bath with Nital. A current density of 3 mA/mm^2 was employed at an applied voltage of 60—70 V. The thinned foils were stored in liquid nitrogen examined in the Hitachi 200-keV electron microscope operating at 200 keV. A double tilting stage was used.

Figure 14 shows the dislocation structure in the (201) plane of the iron single crystal (crystal 1) deformed 2.5% at 200 K. Straight dislocations are aligned parallel to the [111] direction. The Burgers vector of perfect dislocations is of the $(a/2)\langle 111\rangle$ type. The length of any $\langle 100\rangle$ dislocations, formed by interaction between primary and secondary dislocations is very short. The dislocations in Fig. 14 are primarily screw dislocations of the $(a/2)\langle 111\rangle$ type.

The dislocation structure in the (011) plane of crystal 2 is shown in Fig. 15. This photograph is similar to that reported by Spitzig and Thomas[55] for iron deformed at 173 K. Long primary screw dislocations are dominant. The dislocation structure of low-temperature-deformed specimens was observed only in areas probably thicker than 0.3 μm; there is a tendency for dislocations to disappear during thinning preparation of the foil for observation.

The density of dislocations in the cold-rolled specimens

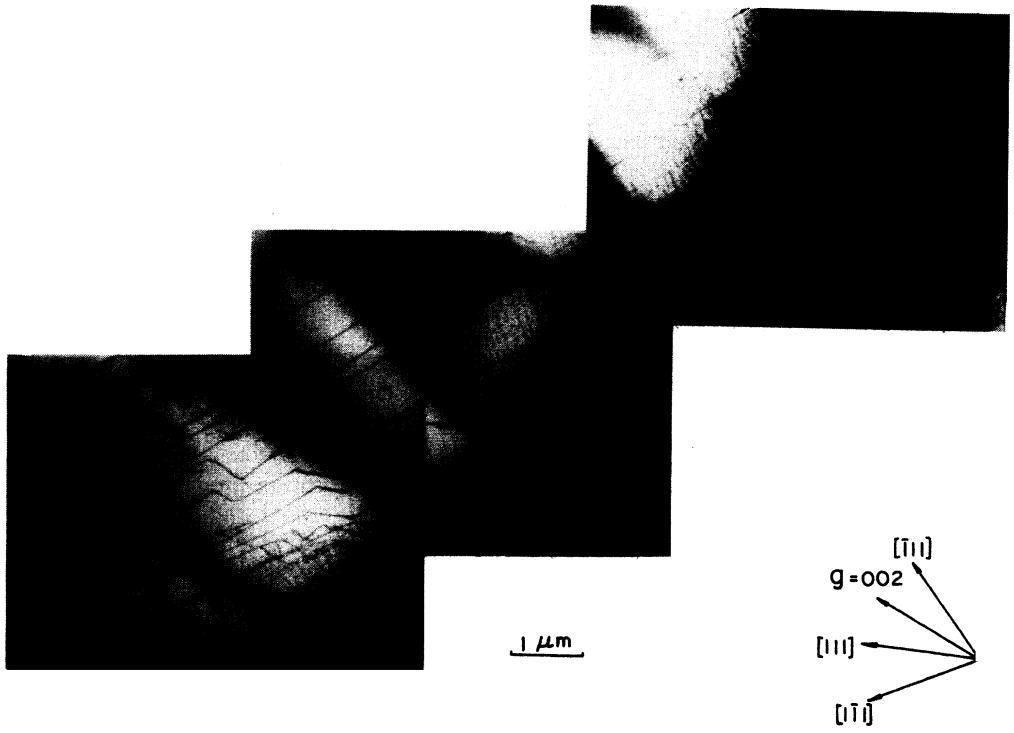

FIG. 14. The dislocation structure in the [201] plane of crystal 1 deformed 2.5% in tension at 200 K. Straight screw dislocations are dominant.

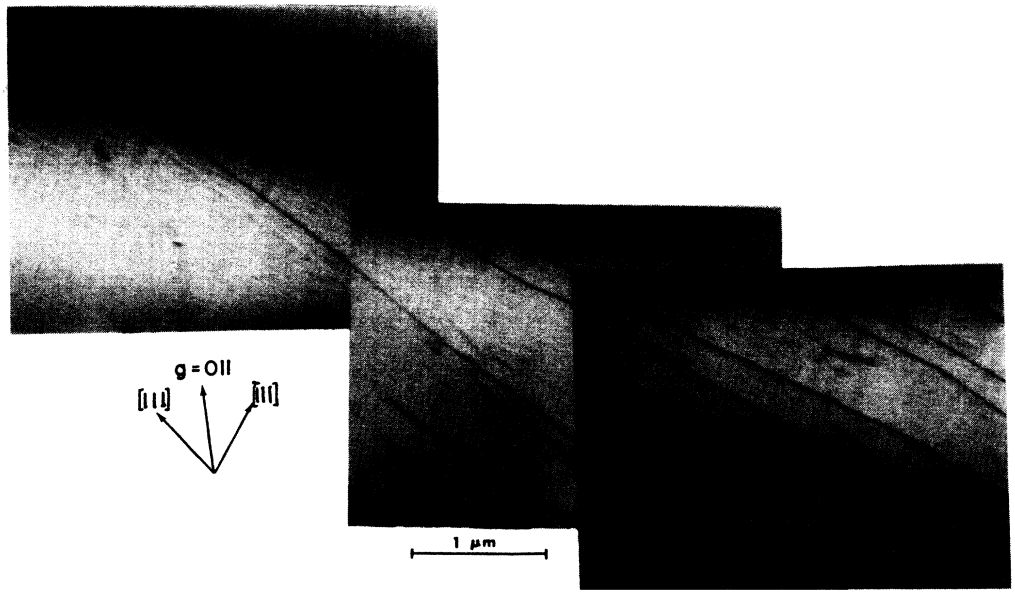

FIG. 15. The dislocation structure in the (001) plane of crystal 2 deformed 5% at 200 K. Long primary screw dislocations of the ⟨111⟩ type are present.

was determined using the method suggested by Keh.[44] The average value can be obtained by counting the number of intersections of dislocation lines with a cross grid. The relation is

$$N=\left[\frac{1}{t}\right]\left[\frac{n_1+n_2}{L_1+L_2}\right],$$

where t is the average thickness of the thin foil, n_1 and n_2 are the number of intersections, and L_1 and L_2 are the total lengths, respectively, of lines 1 and 2. N thus calculated is considered to be the minimum average density because there will be some fraction of the dislocations which are out of contrast due to the microscope's operating condition for the photograph.

The transmission-electron-microscope pictures taken by Kimura and Kimura[36] of lightly deformed single-crystal tensile deformations of similarly oriented iron specimens at 200 K show only relatively simple arrangements of dislocations similar to the present work. The principal defects they observed during small deformations were edge dislocation initially, and then primarily nonkinky screw dislocations of the ⟨111⟩ type. According to Keh and Weissmann[44] the distribution of dislocations is relatively uniform when formed at −75 and −135 °C; cells are not formed below ~16% strain. They arrived at the conclusion that primarily straight screw dislocations of the ⟨111⟩ type were formed up to ~13% strain.

Ikeda[45] studied the dislocation distribution in iron single crystals at 200 K and room temperature. While the transmission electron micrographs were different depending on the orientation of the plane where the micrographs were taken, micrographs taken in the specimens deformed at 200 K by the present authors are similar to Figs. 3(a) and 3(b) of Ikeda; namely, short and straight screw dislocations, with edge-type loops found at low strains (2–6%).

Solomon and McMahon[34] determined the fraction of edge and screw dislocations which were formed in iron single crystals at 77 K. The fraction varied from 40% to 70% screw component depending upon the stress level.

C. Discussing two lifetimes for a dislocation

In a number of earlier studies on deformed iron basically two lifetimes were found: one for annihilation in the bulk and the other for a defect which was most likely a dislocation. Doyama and Cotterill[3] reported 117 and 169 psec, Cao Chuen *et al.*[28] gave 111 and 162 psec, Van Brabander *et al.*[10] reported 108 and 167 psec, and Nielsen *et al.*[56] reported 165 psec for a steel with a longer one attributed to voids.

When first the authors observed the lifetime of 165 psec a significant number of times with carefully bent specimens, (and before we had found the consistent set of lifetimes just cited) Vehanen[22] suggested that this value might well be due to a mixture of traps, one of which was with 157 psec, which the Finnish group had assigned to (undifferentiated) dislocations, and with 175 psec assigned as the lifetime of a monovacancy. As we have seen, his proposal was correct in spirit, but missed the proper identification of the defect species participating in the trapping.

Kuramoto *et al.*[43] carried out very similar deformation of iron single crystals and made positron annihilation measurements. They were convinced *a priori* that dislocations would be very unlikely to be detectable. They annealed their low-temperature deformed specimens for several hours at room temperature. They reported their results in terms of a fixed trap with a lifetime of 175 psec

TABLE V. Results of determining the positron lifetime with one- and two-trap models on specimens deformed at 200 K.

One trap[a]			Two traps[b]		
T (psec)	χ^2/ν	I_2 (%)	T (psec)	χ^2/ν	I_3 (%)
154±3	1.218	78	145±3	1.234	58
153±5	1.180	76	144±4	1.172	56
150±13	1.189	68	140±33	1.189	40
144±14	1.169	72	141±7	1.177	33
148±8	1.514	76	144±10	1.536	49
141±7	1.191	86	137±11	1.175	71
148±8	1.402	72	140±9	1.417	49
157±2	1.553	71	150±8	1.529	43
154±6	1.425	68	147±10	1.426	44
148±10	1.175	77	135±13	1.178	69

[a]The lifetime for annihilation in the bulk was fixed at 114 psec.
[b]Both 114 and 165 psec lifetimes were fixed.

associated with vacancy clusters. They did observe a second lifetime in the vicinity of 350 psec.

Our data were reanalyzed using 175 psec as a fixed lifetime, but we were unable to obtain statistical justification for forcing this value rather than using 165 psec. We did a number of further analyses since we had observed a single-trap lifetime of 155 psec with cold-rolled specimens. The contrary hypothesis occurred to us, namely that since cold rolling takes place with a more complex stress state at various parts of the (single-crystal) sheet, that 155 psec might be due to a mixture of traps. Indeed 165 psec was found together with 143 psec. No strong evidence was obtained for 175 psec after examining a number of carefully deformed specimens. In each case, the χ^2/ν measure of statistical fit was of significantly lower quality using the higher lifetime value.

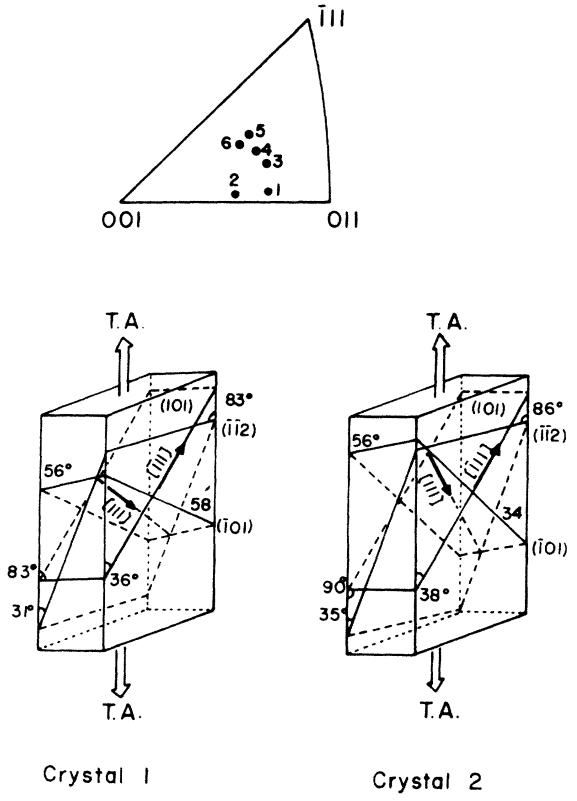

FIG. 16. The orientation of iron single crystals and schematic drawing of the potential slip systems in the tensile specimens with relation to the direction of applied stress. Orientations 3–6 represent the surface normal of the bent and cold-rolled specimens.

The trapping by a mixture of edge and screw dislocations can, in principle, be analyzed with a two-trap model since the two lifetimes were found to be sufficiently well separated for resolution. The number of dislocations with either type of component can thus be obtained. The lifetimes of 114 and 165 psec were fixed and the data were reanalyzed. The values of the lifetime determined in the two ways are presented together with their χ^2/ν values in Table V. In these runs, it was difficult to fit the second trap. Nevertheless, the corresponding values of χ^2/ν in most cases were not significantly different as they would have been if an additional trap was not warranted.

There is another observation of 142 psec for iron; it has been reported by Vehanen *et al.*[57] for a C-vacancy pair. However, this value is not the lifetime of a single type of a trap but rather a "mean" lifetime which comes from assuming only one trapping state. It was resolved by those authors into one component with a lifetime of 160 psec.

D. Related work

Bryne and his co-workers[32] deduced the dislocation content of a heat-treated eutectoid steel from x-ray line

TABLE VI. Schmid factors of slip systems in iron tensile specimens.

Slip direction	Slip plane	Schmid factor Crystal 1	Crystal 2
⟨111⟩	(101)	0.482	0.495
	(211)	0.461	0.433
	(112)	0.383	0.422
⟨111⟩	(101)	0.464	0.485
	(112)	0.380	0.429
	(211)	0.417	0.406

TABLE VII. Effect of the number of traps assumed on the χ^2/ν results for iron single crystals deformed at 200 K.

One trap		Two floating traps			Two traps, one fixed		
T	χ^2/ν	$T^{(1)}$	$T^{(2)}$	χ^2/ν	$T^{(1)}$	Fixed	χ^2/ν
154±3	1.218	147±5	159±7	1.210	145±3	165	1.234
147±4	1.172	139±4	166±13	1.203	138±3	165	1.196
155±5	1.180	145±6	161±9	1.177	144±4	165	1.172
			Average				
152±5		144±6	162±9		142±4	165	

shapes, and measured the Doppler-broadening P/W parameter on the same samples. They concluded that the positrons were annihilating in dislocations within the ferrite grains. It is interesting that they found P/W to yield a straight line when plotted against the dislocation densities in the range of 1×10^{14} m^{-2}. Their value of the specific trapping rate μ_T was 1.5×10^{15} sec^{-1}.

Xiong-Liang-Yue[58] studied the isothermal recrystallization of pure iron which had been rolled to 40% of the original thickness. The change in the dislocation concentration at 500°C was linearly correlated with the volume fraction of newly formed and hence "dislocation-free" grains. There was no change in the R parameter during recrystallization suggesting that there was only one type of positron trap—an undetermined and probably mixed dislocation—involved.

VI. CONCLUSIONS

The consistent behavior of positron annihilation trapping in a fairly large range of deformation experiments on single crystals of high-purity iron has been presented. It has been shown that it is possible to determine the number of screw and edge dislocations per unit area by a combination of the two types of positron annihilation measurements, namely, positron lifetime spectra and line-shape analysis of the Doppler-broadened γ-ray radiation. The number of traps is in good agreement with the density of dislocations revealed by etch pits. Separate specific trapping rates have been determined and compared with similar results which have been published elsewhere.

ACKNOWLEDGMENTS

The assistance and the counsel of Professor I. K. Mackenzie at Guelph University in early stages of this research is gratefully acknowledged. Dr. Wilfred Alsem of Delft University was able to locate and correct an electronic flaw in the operation of the Northwestern University lifetime system. The authors are indebted to him. The authors thank A. Vehanen and B. Neilsen for their helpful discussions. The technical assistance of W. Tremel at Brookhaven National Laboratory is greatly appreciated. Special thanks go to K. G. Lynn for many helpful interactions. In addition long strap-shaped single crystals of high-purity iron were supplied by Professor J. M. T. de Hosson of the University of Groningen, Netherlands. Research was supported by the U. S. Army Research Office and the U. S. Department of Energy, Division of Materials Sciences, Office of Basic Energy Sciences under Contract No. DE-AC02-76CH00016.

APPENDIX A

The orientations of various potential slip planes with respect to the tensile direction are shown in Fig. 16. The appropriate Schmid factors are listed in Table VI.

It can be seen that the slip systems in crystal 1 are more nearly parallel to the wide surface of the tensile specimen. This has an appreciable influence on the dislocations which can remain in the specimen after deformation.

APPENDIX B

A few additional trials at fitting the lifetime data with different choices of the input parameters are shown in Table VII.

The value of χ^2/ν are less sensitive to the choices than had been anticipated. Thus we have adopted the position that the inclusion of the short lifetime or 142 psec is justified since the inclusion of another trap did not worsen the fitting and gave a more consistent interpretation.

[1]I. Ya G. Dekhtyar, D. A. Levine, and V. S. Mikhalenov, Dokl. Akad. Nauk SSSR **156**, 795 (1964) [Sov. Phys.—Dokl. **9**, 492 (1964)].

[2]S. Berko and J. C. Erskine, Phys. Rev. Lett. **19**, 307 (1967).

[3]M. Doyama and R. M. J. Cotterill, in *Proceedings of the 5th International Conference on Positron Annihilation, Japan, 1979,* edited by R. R. Hasiguti and K. Fujiwara (Japan Institute of Metals, Sendai, 1979), p. 89.

[4]J. C. Grosskreutz and W. E. Millet, Phys. Lett. A **28**, 621 (1969).

[5]S. Tanigawa, T. Shinta, and H. Iriyawa, in *Proceedings of the 6th International Conference on Positron Annihilation, Arlington, Texas, 1981,* edited by Paul G. Coleman, Suresh C. Sharma, and Leonard M. Diana (North-Holland, New York, 1982), p. 401.

[6]P. Bergersen and M. J. Stott, Solid State Commun. **7**, 1203 (1969).

[7]P. C. Connors and R. N. West, Phys. Lett. A **30**, 245 (1969).

[8]H. E. Schaefer, P. Valenta, and K. Maier, in *Proceedings of the 5th International Conference on Positron Annihilation, Japan,*

1979, Ref. 3, pp. 509–12.

[9]S. C. Sharma, T. J. Ataiijan, R. M. Johnson, L. M. Diana, S. Y. Chang, and P. G. Coleman, in *Proceedings of the 6th International Conference on Positron Annihilation, Arlington, Texas, 1981,* Ref. 5, p. 401.

[10]P. Van Brabander, D. Segers, M. Dorikens, and L. Dorikens-Vanpraet, *Proceedings of the 6th International Conference on Positron Annihilation, Arlington, Texas, 1981,* Ref. 5, p. 472.

[11]I. K. Mackenzie, Phys. Status Solidi A **12**, K87 (1972).

[12]P. Hautojarvi, A. Vehanen, and V. S. Mikhalenkov, Appl. Phys. **11**, 19 (1976).

[13]P. Hautojarvi, in *Proceedings of the 6th International Conference on Positron Annihilation, Arlington, Texas 1981,* Ref. 5, p. 389.

[14]W. Frank, A. Seeger, and M. Weller, *Proceedings of the 6th International Conference on Positron Annihilation, Arlington, Texas, 1981,* Ref. 5, p. 412.

[15]R. W. Siegel, *Proceedings of the 6th International Conference on Positron Annihilation, Arlington, Texas, 1981,* Ref. 5, p. 351.

[16]C. G. Park, Ph.D. thesis, Northwestern University, 1983.

[17]D. F. Stein, J. R. Low, Jr., and A. U. Seybolt, Acta Metall. **11**, 1253 (1963).

[18]D. J. Quesnel, A. Sato, and M. Meshii, Mater. Sci. Eng. A **18**, 699 (1973).

[19]V. H. C. Crisp, I. K. Mackenzie, and R. N. West. J. Phys. E **6**, 1191 (1973).

[20]B. Nielsen, Ph.D. thesis, Danmarks Tekniske Hijskole, 1978.

[21]M. Eldrup, Y. M. Huang, and B. T. A. McKee, Appl. Phys. **15**, 65 (1978).

[22]A. Vehanen (private communication).

[23]T. M. Hall, Ph.D. thesis, State University of New York at Stony Brook, 1972.

[24]K. G. Lynn (unpublished).

[25]I. K. Mackenzie, N. Thrane, and P. Sen, 4th International Conference on Positron Annihilation, Denmark, 1976 (unpublished), p. 1.

[26]I. K. Mackenzie, in *Positron Solid-State Physics,* proceedings of the "Enrico Fermi" Summer School course on "Positrons in Solids," Varenna, Italy, 1981, edited by W. Brandt and A. Dupasquier (North-Holland, Amsterdam, 1983), p. 1.

[27]B. T. A. McKee, W. Triftshauser, and A. T. Stewart, Phys. Rev. Lett. **28**, 358 (1972).

[28]Cao Chuan, Wang Yun-yu, Xiong Xing-Min, Xiong Liang-yue, and Jiang Jian, in *Proceedings of the 6th International Conference on Positron Annihilation, Arlington, Texas 1981,* Ref. 5, pp. 479–82.

[29]P. J. Schultz, A. Vehanen, W. Thomlinson, K. G. Lynn, and I. K. Mackenzie, J. Phys. F **13**, L265 (1983).

[30]T. M. Hall, A. N. Goland, and C. L. Snead, Jr., Phys. Rev. B **10**, 3062 (1974).

[31]H. H. Jorch and J. L. Campbell, Nucl. Instrum. Methods **143**, 551 (1977).

[32]Po-We Kao, S. Panchanadeeswaran, and J. G. Byrne, Metall. Trans. A **13**, 1177 (1982).

[33]B. Nielsen (private communication).

[34]H. D. Solomon and C. J. McMahon, Jr., *Work Hardening,* edited by J. P. Hirth and J. Weertman (Gordon and Breach, New York, 1966), pp. 311–332.

[35]A. S. Keh, W. A. Spitzig, and Y. Nakada, Philos. Mag. **23**, 829 (1971).

[36]A. Kimura and S. M. Kimura, Mater. Sci. Eng. **58**, 211 (1983).

[37]L. P. Kubin, Rev. Deform. Behavior Mater. **1**, 244 (1976).

[38]Y. T. Chou, Acta. Metall. **13**, 251 (1965).

[39]V. Hibert, P. Groh, P. Moser, and W. Frank, Phys. Status Solidi A **42**, 511 (1977).

[40]R. M. Shemenski, M. H. Beck, and M. G. Fontana, J. Appl. Phys. **216**, 3909 (1965).

[41]K. Yamakawa, T. Tsurata, and S. Yoshikawa, Boshoku Gijutsu **30**, 443 (1981).

[42]K. Yamakawa, T. Tsurata, and S. Yoshikawa, Boshoku Gijutsu **30**, 510 (1981).

[43]E. Kuramoto, Y. Asano, M. Takanaka, and K. Kitajimi, J. Phys. Soc. Jpn. **53**, 1098 (1983).

[44]A. S. Keh and S. Weissmann, in *Electron Microscopy and Strength of Crystals,* edited by G. Thomas and J. Washburn (Interscience, New York, 1963), pp. 231–300.

[45]S. Ikeda, J. Phys. Soc. Jpn. **27**, 1564 (1969).

[46]A. S. Argon and W. C. Moffatt, Acta Metall. **29**, 293 (1981).

[47]L. C. Smedskjaer, M. Manninen, and M. J. Fluss, J. Phys. F **10**, 2237 (1980).

[48]T. Tabata and H. K. Birnbaum, Scripta Metall. **17**, 947 (1983).

[49]T. Tabata and H. K. Birnbaum, Scripta Metall. **18**, 2321 (1984).

[50]C. Huang and I. M. Bernstein, Scripta Metall. **17**, 1299 (1983).

[51](a) C. L. Snead, Jr., K. G. Lynn, Y. Jean, F. W. Wiffen, and P. Schultz, in *Advanced Techniques for Characterizing Microstructures,* edited by F. W. Wiffen and J. A. Spitznagel, Technology of Metallurgy Series (TMS/AIME, Warrendale, PA, 1983), p. 443; (b) P. J. Schultz, K. G. Lynn, I. K. Mackenzie, Y. C. Jean, and C. L. Snead, Jr., Phys. Rev. Lett. **44**, 1629 (1980).

[52]J. R. Low, Jr. and A. M. Turkalo, Acta Metall. **10**, 215 (1962).

[53]J. T. Waber, in *Novel Methods for Materials,* edited by B. B. Rath (The Metallurgical Society Press, Warrendale, Pennsylvania, 1982), pp. 1–44.

[54]G. Adam and M. Delbrück, in *Structural Chemistry and Molecular Biology,* edited by A. Rich and N. Davidson (Freeman, San Francisco, 1968), pp. 198–215.

[55]W. A. Spitzig and L. E. Thomas, Philos. Mag. **25**, 1041 (1972).

[56]B. Nielsen, A. van Veen, L. M. Caspers, W. Lourens, G. Trumpy, and K. Petersen, in *Proceedings of the 6th International Conference on Positron Annihilation, Arlington, Texas, 1981,* Ref. 5, p. 441.

[57]A. Vehanen, P. Hautojarvi, J. Johansson, and J. Yli-Kauppila, Phys. Rev. B **25**, 762 (1982).

[58]Xiong-Lian-Yue, Jiang Jian, Cao Chuan, Wang Yun-Yu, Xiong Xing-Min, in *Proceedings of the 6th International Conference on Positron Annihilation, Arlington, Texas, 1981,* Ref. 5, pp. 476–8.

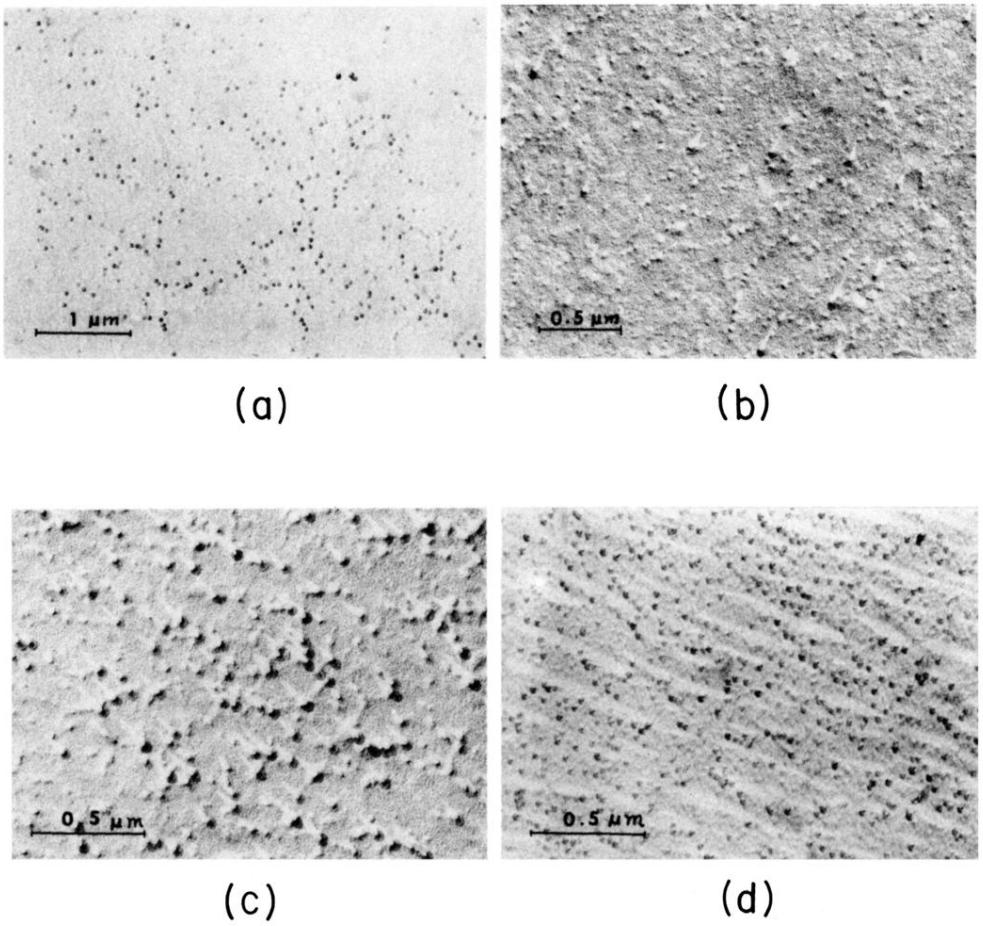

FIG. 11. Transmission electron micrographs of replicas of the etch pits developed on the surface of iron single crystal 1 deformed in tension at 200 K for increasing amounts. (a) $\epsilon=1.0\%$ strain, (b) $\epsilon=2.5\%$, (c) $\epsilon=7\%$, and (d) $\epsilon=9.3\%$.

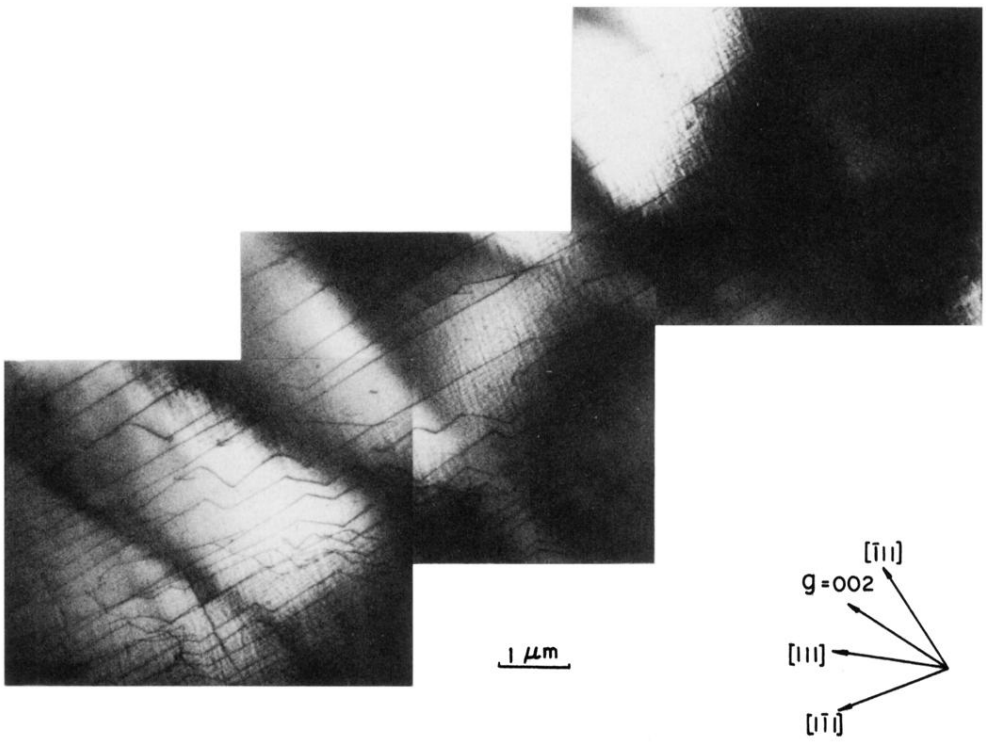

FIG. 14. The dislocation structure in the [201] plane of crystal 1 deformed 2.5% in tension at 200 K. Straight screw dislocations are dominant.

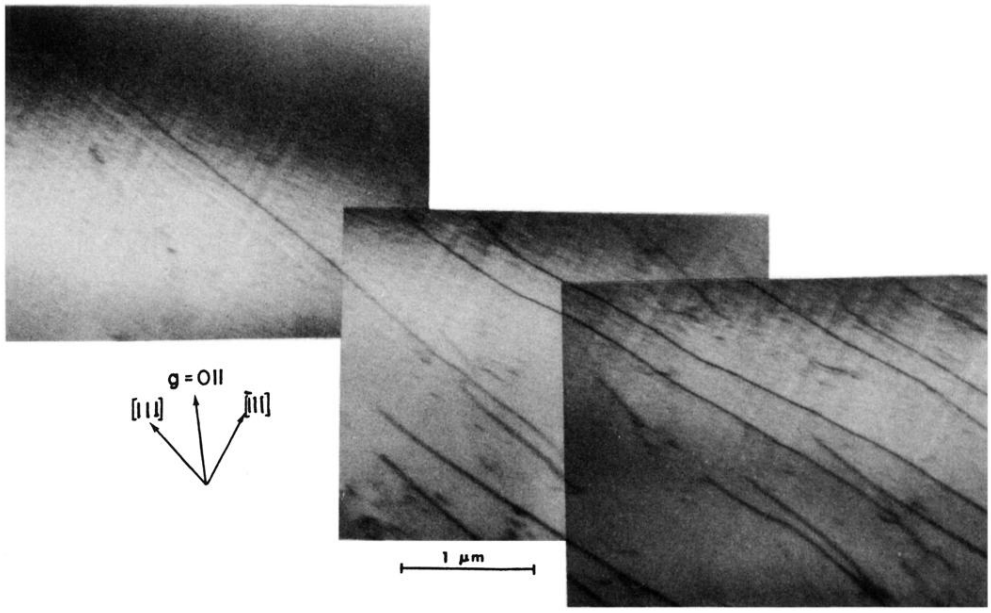

FIG. 15. The dislocation structure in the (001) plane of crystal 2 deformed 5% at 200 K. Long primary screw dislocations of the ⟨111⟩ type are present.